Development and validation of an *in silico* decision-tool to guide optimisation of intravenous artesunate dosing regimens for severe falciparum malaria patients

Sophie G Zaloumis[1], Jason M Whyte[2], Joel Tarning[3,5], Sanjeev Krishna[4], James M McCaw[1,6], Pengxing Cao[6], Michael T White[7], Saber Dini[1], Freya JI Fowkes[1,8], Richard J Maude[3,5,12], Peter Kremsner[9,10], Arjen Dondorp[3,5], Ric N Price[3,5,11] Nicholas J White[3,5] and Julie A Simpson[1]

[1] Centre for Epidemiology & Biostatistics, Melbourne School of Population and Global Health, University of Melbourne, Melbourne, Australia

[2] Centre of Excellence for Biosecurity Risk Analysis, School of BioSciences, University of Melbourne, Melbourne, Australia, and Australian Research Council Centre of Excellence for Mathematical and Statistical Frontiers, School of Mathematics and Statistics, University of Melbourne, Melbourne, Australia

[3] Mahidol-Oxford Tropical Medicine Research Unit, Faculty of Tropical Medicine, Mahidol University, Bangkok, Thailand

[4] Institute for Infection and Immunity, St. George's Hospital, University of London, London, UK

[5] Centre for Tropical Medicine and Global Health, Nuffield Department of Medicine, University of Oxford, Oxford, UK

[6] School of Mathematics and Statistics, University of Melbourne, Melbourne, Australia

[7] Department of Parasites and Insect Vectors, Institut Pasteur, Paris, France

[8] Disease Elimination Program, Burnet Institute, Melbourne, Australia

[9] Centre de Recherches Médicales de Lambaréné, Gabon

[10] Gabon and Institut für Tropenmedizin, University of Tübingen, Germany

[11] Global Health Division, Menzies School of Health Research and Charles Darwin University, Darwin, Northern Territory, Australia

[12] Harvard TH Chan School of Public Health, Harvard University, Boston, USA

*Corresponding author:

Email: sophiez@unimelb.edu.au

Key words: Severe malaria, *Plasmodium falciparum*, intravenous artesunate, pharmacokinetic-pharmacodynamic modelling

ABSTRACT

Most deaths from severe falciparum malaria occur within 24 hours of presentation to hospital. Intravenous (i.v.) artesunate is the first-line treatment for severe falciparum malaria, but its efficacy may be compromised by delayed parasitological responses. In patients with severe malaria the life-saving benefit of the artemisinin derivatives is their ability to clear circulating parasites rapidly, before they can sequester and obstruct the microcirculation. To evaluate the dosing of i.v. artesunate for the treatment of artemisinin-sensitive and reduced ring stage sensitivity to artemisinin severe falciparum malaria infections Bayesian pharmacokinetic-pharmacodynamic modelling of data from 94 patients with severe malaria (80 children from Africa and 14 adults from Southeast Asia) was performed. Assuming delayed parasite clearance reflects a loss of ring stage sensitivity to artemisinin derivatives, the median (95% credible interval) percentage of patients clearing ≥99% parasites within 24 hours (PC24≥99%) for standard (2.4 mg/kg i.v. artesunate at 0 and 12 hours) and simplified (4 mg/kg i.v. artesunate at 0 hours) regimens were 65% (52.5%-74.5%) versus 44% (25%-61.5%) for adults, 62% (51.5%-74.5%) versus 39% (20.5%-58.5%) for larger children (≥20 kg) and 60% (48.5%-70%) versus 36% (20%-53.5%) for smaller children (<20 kg). The upper limit of the credible intervals for all regimens was below a PC24≥99% of 80%, a threshold achieved on average in clinical studies of severe falciparum malaria infections. Rapid clearance of parasites, where there is loss of ring stage sensitivity to artemisinin, in patients with severe falciparum malaria is compromised with the currently recommended and proposed simplified i.v. artesunate dosing regimens.

INTRODUCTION

Despite major advances in malaria control over the last decade, an estimated 405,000 patients died from malaria in 2018 (1). The majority of these deaths are in African children under 5 years of age with *Plasmodium falciparum* malaria (1). Most deaths from severe falciparum malaria occur within the first 24 hours of presentation to a hospital (2). Early diagnosis and treatment with a highly effective antimalarial treatment is key to prevent severe malaria and death (3).

The current global policy for the treatment of both uncomplicated and severe falciparum malaria (referred to as uncomplicated and severe malaria henceforth) relies on the artemisinin derivatives. The World Health Organisation (WHO) treatment guidelines recommend artemisinin combination therapy (ACT) for uncomplicated malaria and intravenous (i.v.) or intramuscular (i.m.) artesunate for severe malaria (3). The reliability and rapid effectiveness of these drugs is now compromised by the emergence of slow clearing parasites with decreased sensitivity to artemisinin derivatives in the Greater Mekong Subregion (4, 5). Optimising the dosing regimens for artemisinin-based therapies is crucial to extend the lifespan of these drugs and prevent the spread of parasites with decreased sensitivity to artemisinin derivatives across Asia and to Africa.

Patients with severe malaria generally have a higher sequestered parasite biomass than those with uncomplicated malaria resulting from efficient multiplication at high densities (8). Decreased sensitivity to artemisinin derivatives is characterised by

delayed parasitological responses (6). The life-saving benefit of the artemisinin compounds in severe malaria results from the rapid killing and clearance of circulating parasites, before they can sequester and obstruct the microcirculation (7). There is also evidence that patients with severe malaria have higher parasite multiplication rates that contribute to the higher biomass found in severe disease, further highlighting the importance of artemisinin derivatives to clear circulating parasites rapidly (8). Hence delayed parasite clearance (reflecting reduced ring stage killing and clearance) is a major concern for the treatment of severe malaria (9).

The WHO treatment guidelines for severe malaria recommend that the artemisinin derivative, artesunate, should be given at 0, 12, and 24, hours and then daily if required at a parenteral dose of 2.4 mg/kg for adults and larger children (≥20 kg) and, because of lower exposures in younger children, at a dose of 3 mg/kg for smaller children (<20 kg) (9). Once the patient can tolerate oral therapy, treatment is completed with 3 days of an ACT. In Africa, a regimen not requiring a 12 hour dose was proposed to have significant practical advantages in resource-poor settings and remote health facilities (10, 11).

The parasite clearance rate is an informative pharmacodynamic variable and *in silico* pharmacokinetic-pharmacodynamic (PK-PD) modelling offers an informative approach to explore new dosing strategies. This approach has been used to simulate parasite clearance within the first 24 hours for patients with severe malaria. Model-based findings suggest that for patients with artemisinin-sensitive infections a simplified regimen of i.m. artesunate (4 mg/kg at 0, 24 and 48 hours) is comparable in efficacy to the WHO regimen (12). Whilst the WHO recommended regimen was

predicted to be less efficacious in patients infected with parasites with decreased artemisinin sensitivity compared to sensitive parasites, the efficacy of the simplified regimen has yet to be evaluated against parasites with decreased artemisinin sensitivity.

In this study, we fitted a within-host PK-PD model within a Bayesian framework to drug concentration and parasite count data from patients with severe malaria treated with two different i.v. artesunate regimens and performed an external validation. Simulations based on the joint posterior distribution of the PK-PD parameters were performed to compare the parasitological outcomes between hypothetical patients with either artemisinin-sensitive or reduced ring stage sensitivity to artemisinin severe falciparum malaria infections.

RESULTS

Parasitaemia (number of parasites / µl of blood) profiles were available for 94 patients with severe malaria (80 children from Africa and 14 adults from Southeast Asia) treated intravenously with 2.4 mg/kg of artesunate. Details of the trials are provided in Table 1 and published reports (10, 13). Since parasite sampling after 48 hours was sparse, parasitaemia profiles were modelled only from data collected up to and including 48 hours (Figure S1(a) and S1(b)). Baseline patient characteristics and the number of blood samples quantifying parasitaemia are summarised in Table 2.

Assessment of model fit and parameter estimation

149 A within-host PK-PD model was incorporated into a Bayesian hierarchical model and
150 fitted to the observed parasitaemia profiles (METHODS and Supplementary Text 1).
151 Definitions for the nine model parameters are provided in Table 3.
152
153 The posterior predictive check (Supplementary Text 2) in Figure 1(a) indicates that
154 the within-host PK-PD model successfully captures the central trend and variability in
155 the observed parasite count profiles.
156
157 The estimates of the population average parameters are presented in Table 4. The
158 average age of the initial parasite load (μ_{IPL}) was 12.95 hours, and the middle 50% of
159 parasites (interquartile range) were aged between 6.16 and 18.17 hours, indicating that
160 on admission infections consisted of parasites predominantly at the ring stage. The
161 time delay before dihydroartemisinin (DHA) concentration levels in plasma reached
162 the malaria parasite in red blood cells (reflected in a hypothetical intraerythrocytic
163 effect compartment) was 3.3 hours ($\log_e 2$ / 0.21). The EC_{50} concentration in the
164 hypothetical compartment was 20.35 ng/ml. Assuming patients are immunologically
165 naïve, the rate of parasite removal resulting from processes other than the drug (δ_P)
166 was 0.06 / hour, that is 6% ($100 \times (1 - e^{-0.06})$) of parasites at each age will be
167 removed every hour independent of treatment. DHA is assumed to kill parasites aged
168 6-44 hours (referred to as DHA's killing window). The maximal killing effect ($k_{\max}$)
169 of DHA was 0.53 / hour. Thus, for every hour that DHA concentrations are much
170 greater than the EC_{50} concentration, the number of parasites within the killing window
171 will be reduced by 41% ($100 \times (1 - e^{-0.53})$).
172

The observed parasitaemia profiles were not informative for estimation of the population average nor individual-specific parasite multiplication factor (PMF). Similarly, the profiles were not informative for estimation of the slope of the *in vivo* concentration-effect curve (γ). For these parameters the prior and marginal posterior distributions were very similar (see Figure S2). The prior distributions for PMF and γ were based on data and parameter estimates from clinical and *in vitro* studies (Table S1). Figure S3 shows how the between subject variability (ω) parameters influence the shape of the marginal densities of the multivariate logistic-normal distribution specified for individual PD parameters.

Parasitological outcome and dosing regimens

The parasitological outcome measure selected for comparing the different i.v. artesunate regimens was clearance of 99% of a patient's admission parasitaemia within 24 hours (PC24≥99%), a measure that has been used previously in non-inferiority clinical trials of parenteral artesunate (10, 11). The 95% credible interval for PC24≥99% simulated from the model contains the observed PC24≥99% of 82% (95% confidence interval (exact method): 70%-90%) for children and 70% (95% confidence interval: 35%-93%) for adults (Figure 1(b)).

The following three dosing regimens were examined in this study:

1. 2.4 mg/kg of i.v. artesunate at 0, 12, and 24, 48 and 72 hours (*standard* regimen).
2. 4 mg/kg of i.v. artesunate at 0, 24 and 48 hours (*simplified* regimen).

3. 3 mg/kg of i.v. artesunate for smaller children (<20 kg) and 2.4 mg/kg for adults and larger children (>20 kg) at 0, 12, and 24, 48 and 72 hours (*revised* regimen).

Before 2015, the "standard" regimen was recommended by the WHO. In 2012, the simplified regimen was examined in a randomised controlled trial (RCT) as an alternative to the standard regimen in resource-poor settings in Africa. In 2015, the standard regimen for children was revised based on pharmacometric modelling (14, 15). The dose for smaller children was increased in the revised regimen to provide comparable drug exposure to adults and larger children. The PC24≥99%, only evaluates the efficacy of the dose(s) administered in the first 24 hours after treatment.

Comparison of dosing regimens

Medians (black dot) and 95% credible intervals (error bars) were used to compare the distribution of PC24≥99% derived from 100 datasets consisting of different hypothetical patient populations: 100 adults, 100 larger children and 100 smaller children (Figure 2). Simulation of hypothetical patients with either artemisinin-sensitive or reduced ring stage artemisinin sensitivity infections was performed. Decreased ring stage artemisinin sensitivity was modelled by shortening the DHA killing window from 6–44 hours to 12–44 hours to mimic a partial (i.e. 6 hour) loss of ring stage activity. The concentration-effect relationship for parasites remaining in the killing window was assumed to be the same as that inferred for artemisinin-sensitive infections.

The DHA concentration profiles for hypothetical adults, larger and smaller children given each dosing regimen are presented in Figure S4. An example of the corresponding parasitaemia profiles is presented in Figure S5.

Artemisinin-Sensitive Infections

The simplified 4 mg/kg i.v artesunate dose group in Kremsner et al. 2012 (10) was used for external validation of the model prediction. External validation focused on whether the model could reproduce the PC24≥99% for the simplified regimen reported in Kremsner et al. 2012 (10) – the parasitaemia profiles from the standard regimen from this study were used for model fitting.

Kremsner et al. 2012 (10) reported that 78% (95% confidence interval: 69%-87%) of patients that received the simplified regimen achieved PC24≥99% and 85% (95% confidence interval: 77%-93%) of patients that received the standard regimen achieved PC24≥99%. A treatment difference of -7.2% was observed between PC24≥99% for the simplified and standard regimens. The corresponding 95% confidence interval ranged from -18.9% to 4.4% and did not include the prespecified noninferiority margin of -20%.

The median (95% credible interval) for PC24≥99% for hypothetical patients with sensitive infections and administered the standard regimen were 86% (75.5%-93.5%) for adults, 83% (72.5%-90.5%) for larger children and 80% (72%-88%) for smaller children (Figure 2, top panel). These 95% credible intervals for hypothetical larger children treated with the standard regimen and for hypothetical smaller children treated with either the standard or revised regimens contain the observed percentage

and 95% confidence interval reported in Kremsner et al. 2012 (10) for the standard regimen.

For the simplified regimen, the median and 95% credible interval derived from the hypothetical children (63.5% (44.5%-80%) for larger children and 58.5% (41%-74%) for smaller children) underestimated the observed PC24≥99% for the children that received the simplified regimen in Kremsner et al. 2012 [8] (i.e. dataset for external validation, Figure 2, top panel).

Decreased ring stage sensitivity to artemisinin

For infections where the killing window was shortened to 12-44 hours to reduce ring stage activity, rapid clearance of such infections appears to be compromised compared to sensitive infections for both the standard (two doses of 2.4 mg/kg of i.v. artesunate at 0 and 12 hours) and simplified (single dose of 4 mg/kg at 0 hours) regimens. The median values (95% credible intervals) for standard and simplified regimens were 65% (52.5%-74.5%) versus 44% (25%-61.5%) for adults, 62% (51.5%-74.5%) versus 39% (20.5%-58.5%) for larger children (≥20 kg) and 60% (48.5%-70%) versus 36% (20%-53.5%) for younger children (<20 kg) (Figure 2, bottom panel). The upper limit of the credible intervals for all regimens was below a PC24≥99% of 80%, a threshold achieved on average in clinical studies of severe falciparum malaria infections (10, 11).

DISCUSSION

Our within-host PK-PD model captures the key features of malaria parasite clearance following the start of antimalarial treatment. The modelled profiles show similar

central trends (lag and decline) and variability in the observed parasitaemia profiles to those observed in African children and Southeast Asian adults who received the 2.4 mg/kg i.v. artesunate dosing regimen in the studies reported by Kremsner et al. 2012 (10) and Maude et al. 2009 (13), respectively (Figure 1). Simulated parasitological outcomes from the model PD parameters were able to reproduce the percentage PC24≥99% observed for the standard 5-dose (i.e. data used for model fitting). In an external validation of the simplified 3-dose i.v. artesunate regimen, based on findings reported in Kremsner et al. 2012 (10), our model underestimated the observed percentage PC24≥99%.

The patient data used for our model predictions were from a setting prior to the decline in efficacy of artemisinin-based therapies being detected in Southeast Asia, consequently inferences based on posterior summaries for the PD parameters are only appropriate for infections with artemisinin sensitive parasites. In this study decreased sensitivity to artemisinin derivatives was modelled by shortening the DHA killing window, i.e. reduced ring stage activity which conforms to the *in vitro* observations of reduced ring stage killing.

A delayed drug killing effect has been observed in *in vitro* (16, 17) and clinical studies for artemisinin derivatives (18, 19). The time delay before DHA plasma concentration had an apparent effect was 3.3 hours in this study, shorter than the 9 hour delay estimated for Cambodian and Thai adults (18) and 5.6 hour delay estimated for adults in Southern Myanmar (19) after treatment with oral artesunate monotherapy. In addition, artemisinin induced growth retardation (20–22) and/or altering of growth patterns (23) were not modelled.

295

296 The within-host PK-PD model described in this study assumed patients were
297 immunologically naïve. This assumption was considered reasonable as the adult
298 patients were from Southeast Asia (a low transmission setting) and a large proportion
299 of the African children were under 5 years (80%). Assuming the patients are
300 immunologically naïve may cause the killing rate of the drug (k_{max}) to be
301 overestimated, as parasite clearance is attributed to drug only and any contribution
302 from the immune response is ignored.

303

304 The model included a parameter to capture drug independent removal of parasites
305 (δ_P) under the assumption patients were immunologically naïve (i.e. due to host-
306 specific processes, such as the finite lifespan of red blood cells) (20, 24). In this study
307 of Southeast Asian adults and predominantly African children, drug independent
308 removal assuming patients were immunologically naïve was inferred to be 6% of
309 parasites every hour.

310

311 The meta-analysis reported by Zaloumis et al. 2014 (14) found similar PK parameters
312 for Southeast Asian adults and Africa children. The PK-PD analysis presented in this
313 study assumed that the decline in parasitaemia after treatment was driven by a
314 patient's PK profile, and hence the PD analysis was not stratified by adult and child
315 patients. Figure S6 illustrates that simulated profiles generated from individual PD
316 parameters derived from the analysis of the pooled PD profiles (i.e. both adults and
317 children) can capture the central trend and variability in the separate adult and child
318 profiles.

319

Estimation of our model parameters was based on data from only 94 patients and focused on the decline in parasitaemia, and not on clinical outcomes, in the initial 24 hours after treatment with intravenous artesunate. Although our model predicts a slower decline in parasitaemia for infections with decreased ring stage sensitivity to artemisinin derivatives in the first 24 hours, this may not translate to poorer clinical outcomes (25). To determine the consequences of delayed parasite clearance on clinical outcomes in severe falciparum malaria patients, studies should also focus on parasitological and clinical outcomes beyond the first 24 hours of treatment.

In silico modelling of artemisinin-resistant severe malaria infections was also investigated in Jones et al. 2019 (12) by assuming early ring stage parasites were insensitive to artesunate. The conclusions in Jones et al. 2019 (12) regarding the efficacy of the standard i.m. dosing regimen for treating resistant infections where the killing window of DHA has been reduced are consistent with ours for i.v. artesunate and suggest that the standard regimen has reduced efficacy against these infections compared to sensitive infections. Our modelling approach differs in the following ways to that adopted in Jones et al. 2019 (12): Bayesian inference was used for parameter estimation, the posterior predictive distribution was used to simulate the parasitological outcome, and the efficacy of the simplified regimen against artemisinin-resistant infections was examined.

In conclusion, our study suggests that in view of the declining efficacy, including recent reports of de novo emergence of *Pfkelch13*-mediated delayed parasite clearance in sub Saharan Africa (26), the previous excellent therapeutic response to intravenous artesunate may be compromised in patients with severe falciparum

345 malaria. In these areas, the clearance of parasites for both the standard and simplified
346 parenteral regimens may be significantly slower. So far, in uncomplicated malaria
347 these delayed parasite clearance phenotypes have not compromised cures with
348 artemisinin containing combinations when the partner drug retains efficacy.
349 Subsequently, trials focusing on both the initial parasitological response and the
350 clinical consequences of delayed parasite clearance in severe falciparum malaria
351 patients should be considered. New antimalarial treatments with ring stage activity are
352 needed in the immediate future.
353

354 **METHODS**

355 **Study population, study design, dosing and blood sampling**

356 The site, study population, design, i.v. artesunate dosing and blood sampling for the
357 determination of DHA concentration and parasitaemia (parasites / µl of blood) for
358 both studies included in the pooled dataset are provided in Table 1.
359

360 **Within-host pharmacokinetic-pharmacodynamic model**

361 The within-host pharmacokinetic-pharmacodynamic (PK-PD) model was previously
362 published in (27, 28) and describes the blood stage of a malaria infection and its
363 response to treatment. In brief, prior to drug administration the initial parasite load
364 (IPL) of each patient is distributed among the 48 hourly age intervals of the *P.*
365 *falciparum* lifecycle according to a truncated normal distribution with location
366 parameter μ^*_{IPL} hours, scale parameter σ^*_{IPL} hours and truncation limits 1 to 48 hours
367 (Supplementary Text 1 equation [S1]). μ_{IPL} and σ_{IPL} are the mean and standard
368 deviation of the truncated parasite age distribution (Supplementary Text 1 equation
369 [S2] and Figure S7). Every hour after treatment the parasites aged 1 to 47 hours are

shifted to the right and become the number of parasites aged 2 to 48 hours. The parasites aged 48 hours are then multiplied by the parasite multiplication factor (PMF, Table 3). This process was repeated for a follow-up time of 48 hours.

The proportion of parasites that survive an hour of treatment with i.v. artesunate is determined by the delayed concentration-effect sigmoid-E_{max} model described in (18) that links the DHA concentration in the central compartment (blood plasma) to a hypothetical effect-site (intraerythrocytic) compartment (Supplementary Text 1 equation [S6]). The model assumes patients are immunologically naive. The rate of parasite removal due to processes other than drug in patients assumed to be immunologically naïve, δ_P, is included in the model (e.g. host-specific processes, such as the lifespan of red blood cells). The PMF is corrected to account for δ_P (Supplementary Text 1 equation [S4]).

After removal of parasites due to drug and drug independent processes, the sum of the simulated number of parasites aged 1 to 26 hours was used to predict the circulating parasitaemia at time points of interest. DHA, the active metabolite of artesunate, was assumed to kill parasites aged 6-44 hours (29). The model does not have an explicit compartment from which parasites "damaged" by drug can either be cleared or recover and returned to the blood circulation (30). Full details of the model are provided in the Supplementary Text 1.

Statistical analysis

The within-host model (Supplementary Text 1) was incorporated into a Bayesian hierarchical model (Supplementary Text 3) which allows the dynamics to vary across

patients and, consequently, the variation in the observed parasitaemia profiles to be modelled. Parasitaemia measurements were natural log ($\log_e$) transformed and assumed to follow a normal distribution where the residual standard deviation varied by observed study. Data below the microscopy limit of detection (50 parasites / μl of blood) were modelled as censored data using the M3 method (31). The prior distribution for the individual-specific PD parameters was assumed to be multivariate normal (MVN) after logistic transformation (32), i.e.

$$\phi_i = \log_e\left(\frac{\theta_i - a}{b - \theta_i}\right) \sim \mathrm{MVN}(\phi, \Omega) \quad [1]$$

where ϕ_i and θ_i denote 9-dimensional vectors of individual-specific PD parameters after and before logistic transformation for the i^{th} individual, and a and b are 9-dimensional vectors containing the lower and upper bounds for each PD parameter provided in Table 4 and also in Table S1 along with a justification for their selection. The mean vector (ϕ) of the MVN distribution in [1] is the logistic transform of a 9-dimensional vector of population average PD parameters (θ), i.e. $\phi = \log_e\left(\frac{\theta - a}{b - \theta}\right)$. The covariance matrix (Ω) was decomposed into a vector of standard deviation parameters and a correlation matrix (see equation [S10] in Supplementary Text 3). The hyperprior distributions for the elements of the mean vector ϕ, standard deviation parameters, correlation matrix and study-specific residual error were normal(0, 1), half-normal(0, 1), Cholesky LKJ correlation distribution (33, 34) with shape parameter equal to 2 and half-Cauchy(0, 5), respectively.

The No U-Turn (NUTS) sampler implemented in the open source software packages RStan 2.18.2 (35) and R 3.4.2 (36) was used to sample the population average PD, individual-specific PD, BSV parameter values and study-specific residual errors from

the posterior distribution. For each model parameter, four Markov chains were initialised using random numbers generated by RStan. The first 1000 parameter values sampled for each chain were discarded as burn-in and an additional 1000 parameter values were sampled and combined, resulting in 4000 samples per parameter for calculation of posterior summaries. The posterior summaries calculated were the median of the 4000 samples for each parameter (posterior median) and 95% credible interval, which is calculated from the 2.5th and 97.5th percentiles of the 4000 samples for each parameter. The credible interval can be interpreted as an interval in which the probability that the unknown parameter lies within is 0.95.

Traceplots were examined to assess whether the 1000 parameter draws from each chain had converged to a common distribution (Figure S8). Convergence was also monitored using the $\hat{R}$ statistic, which is the ratio of the mean of the variances of the samples within each chain to the variance of the pooled samples across chains (34). If all chains have converged to a common distribution, $\hat{R}$ will be one. The effective sample size (ESS) is an estimate of the number of independent draws of the parameter of interest from the posterior distribution (34). The draws within a Markov chain are not independent and if there is high autocorrelation between the draws for a parameter, the ESS will be much smaller than the total sample size (i.e. the 4000 draws retained after burn-in for each parameter). To gauge the degree to which the observed data update the prior information, a comparison of the prior distribution and marginal posterior distribution for the population average PD parameters, between-subject variability and individual-specific PD parameters for an individual is provided in Figure S2. Additional details concerning model building and selection are provided in Supplementary Text 4.

Simulation of PC24≥99% under standard and simplified dosing regimens

PK parameters (clearance (CL) and volume of distribution (V)) were simulated for different hypothetical patient populations (100 adults, 100 larger (≥20 kg) children and 100 smaller (<20 kg) children) from the population PK model for patients that received i.v. artesunate at baseline described in (15). Simulation of individual-specific PK parameters from this model requires age, weight, haemoglobin and body temperature values for each hypothetical patient. There was little correlation between these variables for the 14 adults in the pooled study (all Pearson's correlations below 0.4), so values of these variables for the 100 hypothetical adults were sampled from uniform distributions with limits set to the observed range for each variable: age 21-62 years, weight 33-75 kg, haemoglobin 2.9-11.5 g/dl and temperature 34-39 °C.

For the 80 children in the pooled study, age was correlated with both weight and haemoglobin, but temperature was not strongly correlated with any variable. Five-hundred age and temperature values were sampled from uniform distributions with limits set to the observed range for the 80 children: age 0.5-9.2 years and temperature 35-40 °C. The sampled age values were used to simulate 500 corresponding weight and haemoglobin values using the coefficient estimates from the linear regressions of age and weight (estimated intercept, age coefficient and residual standard error were 7.02, 1.76 and 2.01, respectively), and age and haemoglobin (estimated intercept, age coefficient and residual standard error 5.79, 0.59 and 2.01, respectively) for the 80 children in the study. The age, haemoglobin and temperature values for the first 100 weight values ≥20 kg (<20 kg) were retained and used to simulate PK parameters for larger (smaller) children.

Then for each dosing regimen, the simulated weights and PK parameters for each hypothetical patient were used to calculate the i.v. artesunate dose in μg and to simulate the DHA plasma concentration (ng/ml) from the intravenous-bolus one-compartment PK model described in (15), respectively.

Next, 100 datasets each consisting of 100 hypothetical adults, larger children or smaller children with parasitaemia measurements simulated at 6 hourly intervals for 7 days follow-up, after treatment with each i.v. artesunate dosing regimen, were simulated. The 100 hypothetical datasets were generated from the last 100 of the 4000 draws of ϕ and Ω as defined in [1]. For each patient population 100 vectors of ϕ_i were then sampled from this distribution at each of the 100 draws of ϕ and Ω. The inverse logistic transform $\left(a \times \left(1 - \text{logit}^{-1}(\phi_i)\right)\right) + b \times \text{logit}^{-1}(\phi_i)$, where $\text{logit}^{-1}(x) = 1/(1 + e^{-x})$ and a and b are the lower and upper bounds, respectively, for the PD parameters in Table 4 and Table S1) was then applied to each of the ϕ_i vectors, to obtain individual-specific PD parameters on the original scale and within their biologically plausible bounds. These vectors were then used to simulate parasitaemia profiles from the within-host PK-PD model for each hypothetical patient (Figure S5).

For each dosing regimen examined, the simulated DHA concentration profiles (Figure S4) do not vary between datasets. The individual-specific PD parameters for the hypothetical patients vary between datasets, but not between dosing regimens. Details concerning the calculation of PC24≥99% for hypothetical patients are provided in the Supplementary Text 5. The simulation of parasitaemia profiles for infections with

reduced ring stage sensitivity to artemisinin derivatives required shortening the DHA killing window from 6-44 hours, where the drug is known to have an effect, to 12-44 hours in supplementary equation [S5]. The process outlined above is then repeated for the within-host PK-PD model with shortened DHA killing window.

ACKNOWLEDGEMENTS

We would like to thank staff and patients at Chittagong Medical College Hospital in Bangladesh, Centre de Recherches Médicales de Lambaréné and Université des Sciences de la Santé in Gabon and Queen Elizabeth Central Hospital in Malawi, where the data were collected.

AUTHOR CONTRIBUTIONS

S.G.Z. and J.A.S. wrote the first draft of the manuscript; J.A.S. designed the research with input from R.N.P. and N.J.W.; P.K., S.K., A.D., N.J.W. and R.J.M. contributed the data; S.G.Z., J.M.W. and J.A.S. performed the statistical analysis with guidance from J.M.M, J.T., M.T.W., P.C., S.D. and F.J.I.F. All authors critically reviewed and approved the final version of the manuscript.

CONFLICT OF INTEREST

All authors declared no competing interests for this work.

FUNDING

The work was supported by the National Health and Medical Research Centre (NHMRC) of Australia Project Grant (1025319) and supported in part by the Australian Centre for Research Excellence on Malaria Elimination, funded by the

NHMRC (1134989). S.G.Z. is funded by an Australian Research Council (ARC) Discovery Early Career Researcher Award (170100785), J.A.S. is supported by a NHMRC Senior Research Fellowship (1104975), F.J.I.F. is supported by a NHMRC Career Development Fellowship (1166753), R.N.P. is a Wellcome Trust Senior Research Fellow in Clinical Science (091625) and N.J.W. is a Principal Wellcome Trust Fellow. J.T., R.J.M. and A.D. are supported by the Wellcome Trust as part of the Wellcome Trust–Mahidol University–Oxford Tropical Medicine Research Programme. J.T. and RJM are partly funded from the Bill & Melinda Gates Foundation. J.M.M., P.C. and J.A.S. are supported by an Australian Research Council Discovery Project (170103076). P.K. would like to acknowledge Medicines for Malaria Venture for sponsoring the study described in Kremsner et al. 2012 (10).

REFERENCES

1. WHO. World malaria report 2019. Geneva. 2019.
2. Idro R, Jenkins NE, Newton CR. 2005. Pathogenesis, clinical features, and neurological outcome of cerebral malaria. Lancet Neurol 4:827–840.
3. WHO. Guidelines for the treatment of malaria. Third edition. Geneva. 2015. http://www.who.int/malaria/publications/atoz/9789241549127/en/.
4. WHO. Artemisinin and artemisinin-based combination therapy resistance. Geneva. 2016. http://apps.who.int/iris/bitstream/10665/208820/1/WHO_HTM_GMP_2016.5_eng.pdf?ua=1.
5. Ashley EA, Dhorda M, Fairhurst RM, Amaratunga C, Lim P, Suon S, Sreng S, Anderson JM, Mao S, Sam B, Sopha C, Chuor CM, Nguon C, Sovannaroth S, Pukrittayakamee S, Jittamala P, Chotivanich K, Chutasmit K, Suchatsoonthorn

C, Runcharoen R, Hien TT, Thuy-Nhien NT, Thanh NV, Phu NH, Htut Y, Han K-T, Aye KH, Mokuolu OA, Olaosebikan RR, Folaranmi OO, Mayxay M, Khanthavong M, Hongvanthong B, Newton PN, Onyamboko MA, Fanello CI, Tshefu AK, Mishra N, Valecha N, Phyo AP, Nosten F, Yi P, Tripura R, Borrmann S, Bashraheil M, Peshu J, Faiz MA, Ghose A, Hossain MA, Samad R, Rahman MR, Hasan MM, Islam A, Miotto O, Amato R, MacInnis B, Stalker J, Kwiatkowski DP, Bozdech Z, Jeeyapant A, Cheah PY, Sakulthaew T, Chalk J, Intharabut B, Silamut K, Lee SJ, Vihokhern B, Kunasol C, Imwong M, Tarning J, Taylor WJ, Yeung S, Woodrow CJ, Flegg JA, Das D, Smith J, Venkatesan M, Plowe C V., Stepniewska K, Guerin PJ, Dondorp AM, Day NP, White NJ. 2014. Spread of Artemisinin Resistance in Plasmodium falciparum Malaria. N Engl J Med 371:411–423.

6. Dondorp AM, Nosten F, Yi P, Das D, Phyo AP, Tarning J, Lwin KM, Ariey F, Hanpithakpong W, Lee SJ, Ringwald P, Silamut K, Imwong M, Chotivanich K, Lim P, Herdman T, An SS, Yeung S, Singhasivanon P, Day NPJ, Lindegardh N, Socheat D, White NJ. 2009. Artemisinin Resistance in Plasmodium falciparum Malaria. N Engl J Med 361:455–467.

7. White NJ, Turner GDH, Day NPJ, Dondorp AM. 2013. Lethal Malaria: Marchiafava and Bignami Were Right. J Infect Dis 208:192–198.

8. Kingston HW, Ghose A, Plewes K, Ishioka H, Leopold SJ, Maude RJ, Paul S, Intharabut B, Silamut K, Woodrow C, Day NPJ, Chotivanich K, Anstey NM, Hossain A, White NJ, Dondorp AM. 2017. Disease Severity and Effective Parasite Multiplication Rate in Falciparum Malaria. Open Forum Infect Dis 4:1–4.

9. Phyo AP, Win KK, Thu AM, Swe LL, Htike H, Beau C, Sriprawat K,

Winterberg M, Proux S, Imwong M, Ashley EA, Nosten F. 2018. Poor response to artesunate treatment in two patients with severe malaria on the Thai–Myanmar border. Malar J 17:30.

10. Kremsner PG, Taylor T, Issifou S, Kombila M, Chimalizeni Y, Kawaza K, Bouyou Akotet MK, Duscha M, Mordmüller B, Kösters K, Humberg A, Miller RS, Weina P, Duparc S, Möhrle J, Kun JFJ, Planche T, Teja-Isavadharm P, Simpson JA, Köhler C, Krishna S. 2012. A simplified intravenous artesunate regimen for severe malaria. J Infect Dis 205:312–319.

11. Kremsner PG, Adegnika AA, Hounkpatin AB, Zinsou JF, Taylor TE, Chimalizeni Y, Liomba A, Kombila M, Bouyou-Akotet MK, Mawili Mboumba DP, Agbenyega T, Ansong D, Sylverken J, Ogutu BR, Otieno GA, Wangwe A, Bojang KA, Okomo U, Sanya-Isijola F, Newton CR, Njuguna P, Kazungu M, Kerb R, Geditz M, Schwab M, Velavan TP, Nguetse C, Köhler C, Issifou S, Bolte S, Engleitner T, Mordmüller B, Krishna S. 2016. Intramuscular Artesunate for Severe Malaria in African Children: A Multicenter Randomized Controlled Trial. PLOS Med 13:e1001938.

12. Jones S, Hodel EM, Sharma R, Kay K, Hastings IM. 2019. Optimal Treatments for Severe Malaria and the Threat Posed by Artemisinin Resistance. J Infect Dis 219:1243–1253.

13. Maude RJ, Plewes K, Faiz MA, Hanson J, Charunwatthana P, Lee SJ, Tärning J, Yunus E Bin, Hoque MG, Hasan MU, Hossain A, Lindegardh N, Day NPJ, White NJ, Dondorp AM. 2009. Does artesunate prolong the electrocardiograph QT interval in patients with severe malaria? Am J Trop Med Hyg 80:126–32.

14. Hendriksen I, Mtove G, Kent A, Gesase S, Reyburn H, Lemnge MM, Lindegardh N, Day NPJ, von Seidlein L, White NJ, Dondorp AM, Tarning J.

2013. Population Pharmacokinetics of Intramuscular Artesunate in African Children With Severe Malaria: Implications for a Practical Dosing Regimen. Clin Pharmacol Ther 93:443–450.

15. Zaloumis SG, Tarning J, Krishna S, Price RN, White NJ, Davis TME, McCaw JM, Olliaro P, Maude RJ, Kremsner P, Dondorp A, Gomes M, Barnes K, Simpson JA. 2014. Population Pharmacokinetics of Intravenous Artesunate: A Pooled Analysis of Individual Data From Patients With Severe Malaria. CPT Pharmacometrics Syst Pharmacol 3:145.

16. Cao P, Klonis N, Zaloumis S, Dogovski C, Xie SC, Saralamba S, White LJ, Fowkes FJI, Tilley L, Simpson JA, McCaw JM. 2017. A Dynamic Stress Model Explains the Delayed Drug Effect in Artemisinin Treatment of Plasmodium falciparum. Antimicrob Agents Chemother 61:e00618-17.

17. Klonis N, Xie SC, McCaw JM, Crespo-Ortiz MP, Zaloumis SG, Simpson JA, Tilley L. 2013. Altered temporal response of malaria parasites determines differential sensitivity to artemisinin. Proc Natl Acad Sci 110:5157–5162.

18. Lohy Das J, Dondorp AM, Nosten F, Phyo AP, Hanpithakpong W, Ringwald P, Lim P, White NJ, Karlsson MO, Bergstrand M, Tarning J. 2017. Population Pharmacokinetic and Pharmacodynamic Modeling of Artemisinin Resistance in Southeast Asia. AAPS J 19:1842–1854.

19. Lohy Das JP, Kyaw MP, Nyunt MH, Chit K, Aye KH, Aye MM, Karlsson MO, Bergstrand M, Tarning J. 2018. Population pharmacokinetic and pharmacodynamic properties of artesunate in patients with artemisinin sensitive and resistant infections in Southern Myanmar. Malar J 17:126.

20. Dogovski C, Xie SC, Burgio G, Bridgford J, Mok S, McCaw JM, Chotivanich K, Kenny S, Gnädig N, Straimer J, Bozdech Z, Fidock DA, Simpson JA,

618 Dondorp AM, Foote S, Klonis N, Tilley L. 2015. Targeting the Cell Stress
619 Response of Plasmodium falciparum to Overcome Artemisinin Resistance.
620 PLOS Biol 13:e1002132.
621 21. Cao P, Klonis N, Zaloumis S, Khoury DS, Cromer D, Davenport MP, Tilley L,
622 Simpson JA, McCaw JM. 2017. A mechanistic model quantifies artemisinin-
623 induced parasite growth retardation in blood-stage Plasmodium falciparum
624 infection. J Theor Biol 430:117–127.
625 22. Khoury DS, Cromer D, Elliott T, Soon MSF, Thomas BS, James KR, Best SE,
626 Aogo RA, Engel JA, Gartlan KH, Akter J, Sebina I, Haque A, Davenport MP.
627 2017. Characterising the effect of antimalarial drugs on the maturation and
628 clearance of murine blood-stage Plasmodium parasites in vivo. Int J Parasitol
629 47:913–922.
630 23. Hott A, Casandra D, Sparks KN, Morton LC, Castanares G-G, Rutter A, Kyle
631 DE. 2015. Artemisinin-Resistant Plasmodium falciparum Parasites Exhibit
632 Altered Patterns of Development in Infected Erythrocytes. Antimicrob Agents
633 Chemother 59:3156–3167.
634 24. Cao P, Collins KA, Zaloumis S, Wattanakul T, Tarning J, Simpson JA,
635 McCarthy J, McCaw JM. 2019. Modeling the dynamics of Plasmodium
636 falciparum gametocytes in humans during malaria infection. Elife 8:641472.
637 25. Krishna S, Kremsner PG. 2013. Antidogmatic approaches to artemisinin
638 resistance: reappraisal as treatment failure with artemisinin combination
639 therapy. Trends Parasitol 29:313–317.
640 26. Uwimana A, Legrand E, Stokes BH, Ndikumana J-LM, Warsame M, Umulisa
641 N, Ngamije D, Munyaneza T, Mazarati J-B, Munguti K, Campagne P,
642 Criscuolo A, Ariey F, Murindahabi M, Ringwald P, Fidock DA,

643 Mbituyumuremyi A, Menard D. 2020. Emergence and clonal expansion of in
644 vitro artemisinin-resistant Plasmodium falciparum kelch13 R561H mutant
645 parasites in Rwanda. Nat Med.
646 27. Saralamba S, Pan-Ngum W, Maude RJ, Lee SJ, Tarning J, Lindegårdh N,
647 Chotivanich K, Nosten F, Day NPJ, Socheat D, White NJ, Dondorp AM, White
648 LJ. 2011. Intrahost modeling of artemisinin resistance in Plasmodium
649 falciparum. Proc Natl Acad Sci U S A 108:397–402.
650 28. Zaloumis S, Humberstone A, Charman SA, Price RN, Moehrle J, Gamo-Benito
651 J, McCaw J, Jamsen KM, Smith K, Simpson JA. 2012. Assessing the utility of
652 an anti-malarial pharmacokinetic-pharmacodynamic model for aiding drug
653 clinical development. Malar J 11:303.
654 29. ter kuile F, White NJ, Holloway P, Pasvol G, Krishna S. 1993. Plasmodium
655 falciparum: In Vitro Studies of the Pharmacodynamic Properties of Drugs Used
656 for the Treatment of Severe Malaria. Exp Parasitol 76:85–95.
657 30. White NJ, Watson J, Ashley EA. 2017. Split dosing of artemisinins does not
658 improve antimalarial therapeutic efficacy. Sci Rep 7:7–11.
659 31. Bergstrand M, Karlsson MO. 2009. Handling data below the limit of
660 quantification in mixed effect models. AAPS J 11:371–80.
661 32. Lesaffre E, Rizopoulos D, Tsonaka R. 2007. The logistic transform for
662 bounded outcome scores. Biostatistics 8:72–85.
663 33. Lewandowski D, Kurowicka D, Joe H. 2009. Generating random correlation
664 matrices based on vines and extended onion method. J Multivar Anal
665 100:1989–2001.
666 34. Carpenter B, Gelman A, Hoffman MD, Lee D, Goodrich B, Betancourt M,
667 Brubaker M, Guo J, Li P, Riddell A. 2017. Stan : A Probabilistic Programming

Language. 2.17.0. J Stat Softw 76.

35. Stan Development Team. 2018. RStan: the R interface to Stan. R package version 2.18.2. http://mc-stan.org/.

36. R Core Team. 2019. R: A language and environment for statistical computing. R Foundation for Statistical Computing, Vienna, Austria. https://www.R-project.org/.

FIGURE LEGENDS

Figure 1. Posterior predictive check of the within-host PK-PD model fitted to the observed data (n = 94 patients). In the upper panel of (a), the solid black circles are the observed $\log_{10}$ parasitaemia (parasites / μl of blood), and the following are plotted for bins across the independent variable, time after i.v. artesunate administration: median (middle red dashed line), 5th and 95th percentiles (lower and upper red dashed lines, respectively) of the observed parasitaemia; and 95% credible intervals for the median (red region), 5th and 95th percentiles (blue regions) predicted from the within-host PK-PD model. Dashed horizontal line is the microscopic limit of detection (LOD) of 50 parasites / μl of blood. In the lower panel of (a), the solid black line is the observed fraction of parasite counts at each sampling time below the LOD, and the blue region is the 95% credible interval for the median fraction of below LOD parasitaemia samples predicted from the within-host PK-PD model with noise added. In (b), are the medians (black dot) and 95% credible intervals (error bars) for the percentage of children and adults that cleared 99% of their admission parasitaemia by 24 hours (PC24≥99%) derived from 4000 replicated datasets simulated from the within-host PK-PD model. The observed PC24≥99% derived from the 94 patients was 82% for children and 70% for adults and these are indicated by the black dashed lines.

The grey shaded regions are corresponding 95% confidence intervals: (70%-90%) for children and (35%-93%) for adults.

Figure 2. Comparison of the median (black dot) and 95% credible interval (error bars) for the PC24≥99% achieved by hypothetical adults, larger (≥20 kg) and smaller (<20 kg) children. PC24≥99% calculated from 100 datasets consisting of simulated parasitaemia profiles for 100 adults, 100 larger children and 100 smaller children, with either artemisinin sensitive (top) or reduced ring stage sensitivity to artemisinin (bottom row is DHA killing window shortened from 6-44 hours to 12-44 hours) infections, administered the standard (2.4 mg/kg of i.v. artesunate at 0, 12, and 24, 48 and 72 hours), revised (3 mg/kg of i.v. artesunate for smaller children (<20 kg) and 2.4 mg/kg for adults and larger children (>20 kg) at 0, 12, and 24, 48 and 72 hours) and simplified (4 mg/kg of i.v. artesunate at 0, 24 and 48 hours) dosing regimens. The black and purple dashed lines are the percentage PC24≥99% for the conventional 5-dose regimen of 2.4 mg/kg i.v. artesunate (standard regimen) and simplified 3-dose regimen of 4 mg/kg i.v. artesunate (simplified regimen) reported in Kremsner et al. 2012 (10) (85% and 78%, respectively) and the black and purple regions are the corresponding 95% confidence intervals (77%–93%) and (69%–87%), respectively.

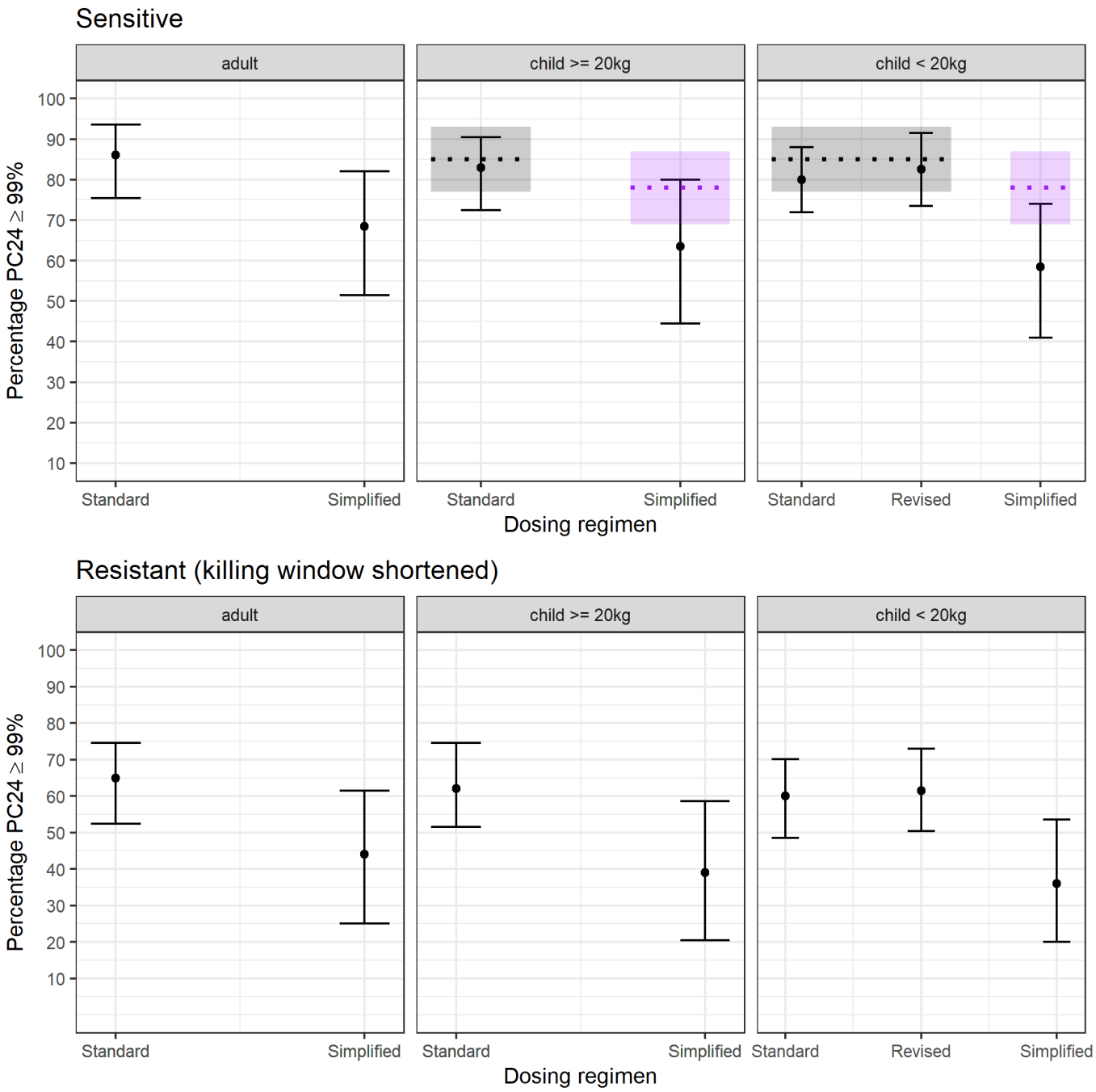

Table 1. Study site, population, design, dosing scheme and parasitaemia sampling times for each study.

Research Team	Kremsner et al. 2012 (10)	Maude et al. 2009 (13)
Site	Gabon, Malawi	Bangladesh
Population	Children with severe malaria	Adults with severe malaria
Design	Randomised Controlled Trial	Clinical Study
Dosing regimen	I – 2.4 mg/kg i.v. at 0, 12, 24, 48, 72 h[a] II – 4 mg/kg IV at 0, 24, 48 h	2.4 mg/kg i.v. at 0, 12, 24 and then every 24 h as required
Sampling times		
ARS/DHA concentration	2 samples/patient taken from times[b] 0.083, 0.167, 0.25, 0.5, 1, 2, 4, and 6 h	0, 0.167, 0.5, 1, 2, and 4 h
Parasitaemia	0, 6, 12, 18, 24 h and then every 6 h until there were 2 consecutive negative[c] slides	0, 1, 2, 3, 4, 5, 6, 8, 10, 12, 18, 24 h and then every 6 h until parasite clearance

[a]Only these patients included in the analysis

[b]Patients randomly allocated to one of eight different sampling groups where each sampling group has two time points (e.g. group 1–5 min, 2 h post first dose).

[c]Negative slide defined as number of circulating parasitized blood cells below the limit of detection (50 parasites / µl of blood).

Table 2. Summary of the number of blood samples for parasitaemia measurement, including the number of samples below the microscopic limit of detection (LOD), and baseline patient characteristics for each study.

Research Team	Kremsner et al. 2012 (10)	Maude et al. 2009 (13)
No. patients	80	14
No. male	44	11
No. samples	463	87
No. below LOD[a]	68	5
Median samples per patient [range]	6 [2, 9]	11 [1, 14]
Baseline patient characteristics[b]		
Median Parasitaemia (parasites / µl of blood)	214,824 [869 to 1,870,264]	92,630 [22,608 to 534,554]
Age (years)	3 [0.6 to 9.3]	37.5 [22 to 62]
Weight (kg)	12 [6 to 24]	60 [33 to 75]

[a]LOD – Limit of detection for microscopic blood film examination: 50 parasites / µl of blood

[b] Median [Range]

Table 3. Parameter definitions for the within-host pharmacokinetic-pharmacodynamic model.

Parameter	Description
IPL	Initial parasite load of patient on admission
μ^*_{IPL}	Mean of the age distribution of the initial parasite load (hours) before truncation (normal).
μ_{IPL}	Mean of the age distribution of the initial parasite load (hours) after truncation (truncated normal).
σ^*_{IPL}	Standard deviation of the age distribution of the initial parasite load (hours) before truncation (normal).
σ_{IPL}	Standard deviation of the age distribution of the initial parasite load (hours) after truncation (truncated normal).
PMF	Parasite multiplication factor. Number of parasites released by a ruptured schizont at the end of the lifecycle.
k_{max}	Maximal killing rate of the drug (/ hour)
EC_{50}	*In vivo* concentration when killing rate is 50% of k_{max} (ng/ml)
γ	Slope of *in vivo* concentration-effect curve
k_{e0}	Rate the drug moves from the central compartment (blood plasma) to a hypothetical effect-site (intraerythrocytic compartment) (/ hour)
δ_P	Rate of parasite removal due to processes other than drug (/ hour). Patients are assumed to be immunologically naïve.

Antimicrobial Agents and Chemotherapy

Table 4. Posterior summaries for the population mean pharmacodynamics (PD) parameters, between subject variability (BSV) and study-specific residual errors calculated from 4000 draws from the posterior distribution.

Parameter	Bounds[a]	Posterior median (95% credible interval)	ESS[b]	$\hat{R}$[c]
Population average PD parameter[d]				
IPL (no. of parasites)	(8.69×10^{9},1.870264×10^{13})	2.8×10^{11} (1.9×10^{11}, 4×10^{11})	668	1.01
μ^{*}_{IPL}(hr)	(1,48)	5.41 (2.49, 11.39)	689	1
μ_{IPL}(hr)		12.95 (11.53, 15.90)		
σ^{*}_{IPL}(hr)	(4,14)	12.74 (11.75, 13.46)	1839	1
σ_{IPL}(hr)		8.47 (7.73, 9.51)		
PMF	(5,20)	11.39 (6.47, 17.75)	2379	1
$k_{max}(hr^{-1})$	(0.26,1)	0.53 (0.47, 0.6)	342	1.01
EC_{50}(ng/ml)	(1.44,533)	20.35 (7.97, 41.26)	756	1.01
γ	(1,13)	7.14 (2.74, 11.51)	2893	1
k_{e0} (hr^{-1})	(0.01,10)	0.21	728	1

		(0.11, 0.33)		
δ_p (hr^{-1})	(0.001,0.1)	0.06	744	1
		(0.02, 0.09)		
Between subject variability (ω)[e]				
ω_{IPL}		1.51		
		(1.23, 1.86)	1475	1
$\omega_{\mu_{IPL}}$		0.37		
		(0.02, 1.01)	1022	1
$\omega_{\sigma_{IPL}}$		1.76		
		(1.02, 2.78)	306	1.01
ω_{PMF}		0.63		
		(0.03, 2.14)	2468	1
$\omega_{k_{min}}$		1.09		
		(0.81, 1.45)	675	1.01
ω_{EC50}		0.58		
		(0.04, 1.25)	717	1
ω_{γ}		0.63		
		(0.03, 2.13)	3498	1
$\omega_{k_{e0}}$		0.4		
		(0.04, 1.01)	392	1.01
$\omega_{k_{min}}$		0.42		
		(0.02, 1.81)	469	1
Study-specific residual error (σ)				
σ_1		0.95		
		(0.86, 1.05)	1439	1

σ_2		0.69 (0.56, 0.89)	745	1.01

[a]A justification for the bounds is provided in supplementary Table S1.

[b]Effective sample size (ESS) is the number of independent draws of the parameter of interest from the posterior distribution (see METHODS).

[c]If all chains have converged to a common distribution $\hat{R}$ will be one, otherwise it will be greater than one (see METHODS).

[d]Prior to drug administration the initial parasite load (IPL) of each patient is distributed among the 48 hourly age intervals of the *P. falciparum* lifecycle according to a truncated normal distribution with location parameter μ^*_{IPL} hours, scale parameter σ^*_{IPL} hours and truncation limits 1 to 48 hours (Supplementary Text 1 equation [S1]). μ_{IPL} and σ_{IPL} are the mean and standard deviation of the truncated parasite age distribution. Definitions for the nine model parameters are provided in Table 3.

[e]Between subject variability (BSV) is the population standard deviation of the individual PD parameters on the logistic transform scale (see METHODS equation [1]). BSV was only included on μ^*_{IPL} and σ^*_{IPL} not the resulting mean and standard deviation of the truncated age distribution.